

Crucial Role of Cu–S Bonding for Structural Changes Accompanying the Reversible Cu^I/Cu^{II} Transition in an Unrestrained Cu(N \wedge S)₂ Coordination Arrangement. An Experimental and DFT Study

Markus Albrecht,[†] Klaus Hübler,[†] Stanislav Zalis,[‡] and Wolfgang Kaim^{*,†}

Institut für Anorganische Chemie, Universität Stuttgart, Pfaffenwaldring 55, D-70550 Stuttgart, Germany, and J. Heyrovsky Institute of Physical Chemistry, Academy of Sciences of the Czech Republic, Dolejškova 3, CZ-18223 Prague, Czech Republic

Received January 5, 2000

The structure of reversibly oxidizable [Cu(mmb)₂](BF₄) with 1-methyl-2-(methylthiomethyl)-1*H*-benzimidazole (mmb) as bidentate N,S-donor ligand has been determined and compared with that of the copper(II) species [Cu(mmb)₂(η^1 -ClO₄)](ClO₄). In the complex ions of the equilibrium [Cu^I(mmb)₂]⁺ + ClO₄⁻ \rightleftharpoons e⁻ + [Cu^{II}(mmb)₂(η^1 -ClO₄)]⁺ the almost linear N–Cu–N backbone is invariant whereas the bonds to the thioether sulfur centers and especially the changing S–Cu–S angle (145.18(5)° for the Cu^{II} species, 109.33(3)° for the Cu^I form) reflect the metal oxidation state. In contrast to the perchlorate coordinating copper(II) species, [Cu^I(mmb)₂](BF₄) contains a cation with a very large vacant site at the metal center, resulting in elliptical channels within the crystal. DFT calculations on [Cu^I(mb)₂]⁺, [Cu^{II}(mb)₂]²⁺, and [Cu^{II}(mb)₂(OCIO₃)]⁺ with mb = 2-methylthiomethyl-1*H*-benzimidazole confirm the essential role of the metal–sulfur bonds in responding to the reversible Cu^{I/II} electron transfer process, even in the absence of electronically stronger interacting thiolate sulfur centers or sophisticated oligodentate ligands.

Introduction

The very different coordination preferences of copper(I) with its d¹⁰ configuration (linear, trigonal-planar, or tetrahedral geometry) and the prototypical Jahn–Teller ion Cu²⁺ (d⁹ configuration: square-planar or square-pyramidal coordination) have long been associated with the unusually large reorganization effects observed for Cu^I/Cu^{II} transitions in complexes [CuL_m]ⁿ⁺.¹ The biochemical occurrence of this couple in “blue copper” proteins and “type 1” copper-containing enzymes has therefore received special attention;^{2–4} the rapid electron transfer observed there has been attributed to an enforced geometry (“entatic state”), representing a compromise between the Cu^I and Cu^{II} energy minimum coordination structures.⁴

The type 1 copper centers exhibit one cysteinate and two histidine residues as the invariable primary coordination sphere and an additional, more weakly bonded ligand, usually the thioether part of methionine.² Native systems, mutants, and

several model compounds of varying degrees of sophistication have been studied in the past decades;^{2,3,5,6} however, the approach⁶ to use polychelate or bulky ligands to restrict the degrees of freedom (and ensure stability) could not by its very nature fully elucidate the intrinsic coordination change for a reversible Cu^I/Cu^{II} transition with an N₂S₂ set of donor atoms. We now present a rather straightforward model system with just bidentate ligands which allows for more geometrical freedom but shows surprising conceptual parallels to what is known of the biological systems.

The 1-methyl-2-(methylthiomethyl)-1*H*-benzimidazole (mmb) ligand has been recently used in copper chemistry to effect a remarkable valence tautomerism which bears some resemblance to physiologically essential phenomena in amine oxidase enzymes.⁷ Mimicking one histidine and one methionine binding site, the neutral mmb ligand can form five-membered chelate rings with metal centers.^{8,9} The benzimidazole N and thioether S donor atoms are both weakly π accepting but of different “softness”, so that both Cu^I and Cu^{II} complexes can form; crystal

[†] Institut für Anorganische Chemie.

[‡] J. Heyrovsky Institute.

- (1) (a) Krylova, K.; Kulatilleke, C. P.; Heeg, M. J.; Salhi, C. A.; Ochrymowycz, L. A.; Rorabacher, D. B. *Inorg. Chem.* **1999**, *38*, 4322. (b) Ambundo, E. A.; Deydier, M.-V.; Grall, A. J.; Aguera-Vega, N.; Dressel, L. T.; Cooper, T. H.; Heeg, M. J.; Ochrymowycz, L. A.; Rorabacher, D. B. *Inorg. Chem.* **1999**, *38*, 4233 and literature cited.
- (2) (a) Shepard, W. E. B.; Anderson, B. F.; Lewandoski, D. A.; Norris, G. E.; Baker, E. N. *J. Am. Chem. Soc.* **1990**, *112*, 7817. (b) LaCroix, L. B.; Randall, D. W.; Nersissian, A. M.; Hoitink, C. W. G.; Canters, G. W.; Valentine, J. S.; Solomon, E. I. *J. Am. Chem. Soc.* **1998**, *120*, 9621.
- (3) Guckert, J. A.; Lowery, M. D.; Solomon, E. I. *J. Am. Chem. Soc.* **1995**, *117*, 2817.
- (4) (a) Williams, R. J. P. *Inorg. Chim. Acta Rev.* **1971**, *5*, 137. (b) Kaim, W.; Schwederski, B. *Bioinorganic Chemistry*; Wiley: Chichester, 1994; p 22 and 196. (c) Kaim, W.; Rall, J. *Angew. Chem.* **1996**, *108*, 47; *Angew. Chem., Int. Ed. Engl.* **1996**, *35*, 43.
- (5) Di Bilio, A. J.; Hill, M. G.; Bonander, N.; Karlsson, B. G.; Villahermosa, R. M.; Malmström, B. G.; Winkler, J. R.; Gray, H. B. *J. Am. Chem. Soc.* **1997**, *119*, 9921 and literature cited.
- (6) (a) Schilstra, M. J.; Birker, P. J. M. W. L.; Verschoor, G. C.; Reedijk, J. *Inorg. Chem.* **1982**, *21*, 2637. (b) Bouwman, E.; Driessen, W. L.; Reedijk, J. *Coord. Chem. Rev.* **1990**, *104*, 143. (c) Kitajima, N.; Fujisawa, K.; Tanaka, M.; Moro-oka, Y. *J. Am. Chem. Soc.* **1992**, *114*, 9232. (d) Malachowski, M. R.; Adams, M.; Elia, N.; Rheingold, A. L.; Kelly, R. S. *J. Chem. Soc., Dalton Trans.* **1999**, 2177.
- (7) (a) Rall, J.; Wanner, M.; Albrecht, M.; Hornung, F. M.; Kaim, W. *Eur. J. Chem.* **1999**, *5*, 2802. (b) Rall, J.; Wanner, M.; Albrecht, M.; Hornung, F. M.; Kaim, W. *J. Inorg. Biochem.* **1999**, *74*, 187.
- (8) Albrecht, M.; Hübler, K.; Scheiring, T.; Kaim, W. *Inorg. Chim. Acta* **1999**, *287*, 204.
- (9) Albrecht, M.; Scheiring, T.; Sixt, T.; Kaim, W. *J. Organomet. Chem.* **2000**, *596*, 84.

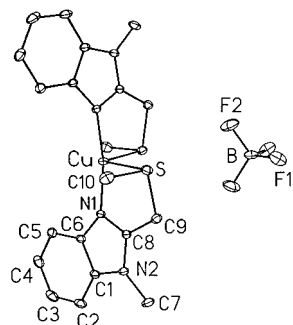


Figure 1. Molecular structure of $[\text{Cu}^{\text{I}}(\text{mmb})_2](\text{BF}_4)$.

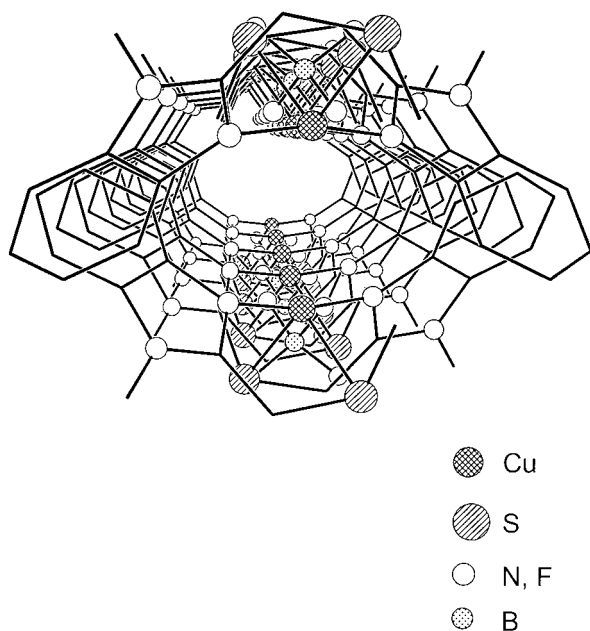
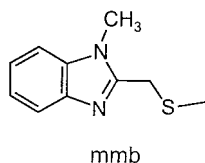


Figure 2. View along the channel formed by the coordinatively unsaturated cations in the crystal of $[\text{Cu}^{\text{I}}(\text{mmb})_2](\text{BF}_4)$.

structures of $[\text{Cu}^{\text{I}}(\text{mmb})(\text{PPh}_3)_2](\text{BF}_4)$ and of poorly soluble $[\text{Cu}^{\text{II}}(\text{mmb})_2(\eta^1\text{-ClO}_4)](\text{ClO}_4)$ were reported recently.⁸

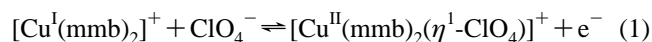


Results and Discussion

Although the new copper(I) species $[\text{Cu}(\text{mmb})_2](\text{BF}_4)$ proved to be a very air-sensitive substance, we were able to determine its crystal structure (Figures 1 and 2, Tables 1 and 2) and study its electrochemistry.

Complex $[\text{Cu}(\text{mmb})_2](\text{BF}_4)$ undergoes electrochemically reversible reduction at 0.31 V vs $\text{FcP}_2^{+/0}$ in noncoordinating $\text{CH}_2\text{Cl}_2/0.2 \text{ M Bu}_4\text{NPF}_6$. The peak-to-peak potential differences between 70 mV at 20 mV/s and 113 mV at 1 V/s scan rate coincide with that of the internal ferrocene standard and thus imply rather little geometrical reorganization,¹ in contrast to the behavior of many other simple complexes of the $\text{Cu}^{\text{I}}/\text{Cu}^{\text{II}}$ couple.

The structural comparison in Table 2 of the complex ions in the equilibrium



reveals the following features:

Table 1. Crystallographic Data for $[\text{Cu}(\text{mmb})_2](\text{BF}_4)$

empirical formula	$\text{C}_{20}\text{H}_{24}\text{BCuF}_4\text{N}_4\text{S}_2$	fw	534.90
cryst syst	monoclinic	space group	$C2/c$
a , Å	18.910(2)	T , K	173
b , Å	10.0519(11)	λ , Å	0.71073
c , Å	12.8339(12)	ρ_{calc} , g cm^{-3}	1.553
β , deg	110.301(7)	μ , mm^{-1}	1.185
V , Å ³	2288.0(4)	$R1^a$	0.0399
Z	4	$wR2^a$	0.0947

$$^a R1 = (\sum||F_o| - |F_c||)/\sum|F_o|, \quad wR2 = \{\sum[w(|F_o|^2 - |F_c|^2)^2]/\sum[w(F_o^4)]\}^{1/2}.$$

Table 2. Comparison of Structural Data

	$[\text{Cu}^{\text{I}}(\text{N}\wedge\text{S})_2]^+$		$[\text{Cu}^{\text{II}}(\text{N}\wedge\text{S})_2(\text{ClO}_4)]$		$[\text{Cu}^{\text{II}}(\text{N}\wedge\text{S})_2]^{2+}$
	exptl ^a	calcd ^b	exptl ^c	calcd ^b	calcd ^b
	Bond Lengths (Å)				
Cu–N	1.9199(18)	1.963	1.941(3)	2.011	1.957
			1.949(3)	2.024	
Cu–S	2.6216(7)	2.711	2.4193(13)	2.599	2.550
			2.4436(13)	2.634	
Cu–O			2.236(9)	2.108	
	Bond Angles (deg)				
N–Cu–N'	169.75(11)	166.3	172.53(14)	164.68	162.6
S–Cu–S'	109.33(3)	112.2	145.18(5)	136.40	120.0
N–Cu–S ^d	82.47(6)	81.8	83.07(11)	80.65	83.2
			83.56(11)	81.48	
N–Cu–S ^e	103.56(6)	106.9	92.31(10)	90.67	106.1
			96.86(11)	95.86	

^a From crystal structure of tetrafluoroborate ($\text{N}\wedge\text{S} = \text{mmb}$). ^b $\text{N}\wedge\text{S} = \text{mb}$. ^c From crystal structure of perchlorate salt (hemimethanolate, $\text{N}\wedge\text{S} = \text{mmb}$), see ref 8. ^d Intrachelate angles. ^e Extrachelate angles.

(i) The N–Cu–N backbone is essentially invariant, because that almost linear arrangement can be part of several ideally preferred structures, whether the linear geometry of copper(I) systems or the square-pyramidal or trigonal-bipyramidal structures of Cu^{II} . In fact, the metal coordination geometry in $[(\text{Cu}^{\text{II}}(\text{mmb})_2(\eta^1\text{-ClO}_4))]^+$ lies midway between the sp and tbp situations,⁸ giving rise to a large value $g_{\parallel} = 2.358$ and a small EPR coupling constant $A_{\parallel} = 13.4 \text{ mT}$.⁸ In contrast, $[\text{Cu}^{\text{I}}(\text{mmb})_2]^+$ exhibits a “2 + 2” coordination with primary N (linear) and secondary S coordination (distorted tetrahedral arrangement) to copper(I).

(ii) The bonds to the thioether sulfur centers reflect the changes at the metal, i.e., the higher ionization of Cu^{II} (causing ca. 7% shorter Cu–S distances) and the capacity for π back-donation from Cu^{I} to the weakly π acidic thioether atoms. A qualitatively similar situation as for $[\text{Cu}^{\text{I}}(\text{mmb})_2](\text{BF}_4)$ had been observed previously for $[\text{Cu}^{\text{I}}(\text{BBDHp})(\text{X})]$, $\text{X} = \text{PF}_6, \text{BF}_4,$ or ClO_4 , in which the tetradentate 1,7-bis(2-benzimidazolyl)-2,6-dithiaheptane (BBDHp) ligand resembles a doubled N–S system as used here.^{6a,10} However, the significantly longer Cu–S distances of about 2.88 Å in these systems indicate rather weak bonding, probably caused by the conformational restraints after formation of the macrocyclic chelate ring. The 2.62 Å distances found for the Cu–S bonds in $[\text{Cu}^{\text{I}}(\text{mmb})_2](\text{BF}_4)$ are shorter than most copper/thioether distances in type 1 Cu centers;^{2,3} a comparable value of 2.61 Å has been reported for the copper(II) state of cucumber basic protein.¹¹

(iii) The distinctly changed S–Cu–S angle reflects the limits of the compromise situation: The large value of 145° for the

(10) Carballo, R.; Castiñeiras, A.; Hiller, W.; Strähle, J. *Acta Crystallogr.* **1991**, *C47*, 1736.

(11) (a) Guss, J. M.; Bartunik, H. D.; Freeman, H. C. *Acta Crystallogr.* **1992**, *B48*, 790. (b) Guss, J. M.; Merritt, E. A.; Phizackerley, R. P.; Freeman, H. C. *J. Mol. Biol.* **1996**, *262*, 686.

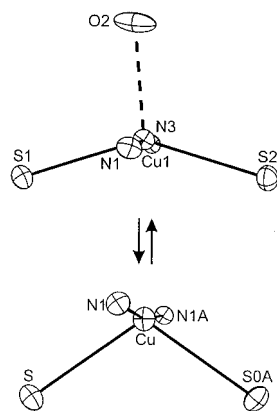


Figure 3. Projections of the coordination arrangements of $[\text{Cu}^{\text{I}}(\text{mb})_2]^+$ (bottom) and $[\text{Cu}^{\text{II}}(\text{mb})_2(\eta^1\text{-OCIO}_3)]^+$ (top) in the CuS_2 plane.

copper(II) complex signifies the “flattening” tendency toward a planar situation for the $\text{Cu}^{\text{II}}\text{N}_2\text{S}_2$ core, whereas the angle of 109.3° for the copper(I) complex would be close to the ideal value in a tetrahedral situation (Figure 3).

(iv) The coordinative unsaturation of the primary $\text{Cu}^{\text{II}}\text{N}_2\text{S}_2$ coordination allows for addition of a fifth, weakly bonded ligand, here $\eta^1\text{-ClO}_4^-$. Similarly, in type 1 copper centers the $\text{Cu}^{\text{II}}(\text{His})_2(\text{Cys}^-)$ primary coordination sphere is usually complemented by methionine and, in some cases, by a very weakly coordinated fifth O-donor ligand.^{2,3} The large vacant site at the very unusually coordinated Cu^{I} center in $[\text{Cu}(\text{mmb})_2]^+$ explains the high air sensitivity in solution and in the solid: Remarkably, the molecules pack with the open coordination sites directed at each other to form approximately elliptical channels in the crystal with axes of about 3.5 and 5.1 Å (Figure 2).

DFT calculations¹² were performed for the $[\text{Cu}^{\text{I}}(\text{mb})_2]^+$, $[\text{Cu}^{\text{II}}(\text{mb})_2]^{2+}$, and $[\text{Cu}^{\text{II}}(\text{mb})_2(\eta^1\text{-ClO}_4)]^+$ ions (mb = 2-(methylthiomethyl)-1*H*-benzimidazole). The $[\text{Cu}^{\text{II}}(\text{mb})_2]^{2+}$ ion was studied because the oxidation of $[\text{Cu}^{\text{I}}(\text{mmb})_2](\text{BF}_4)$ primarily produces a tetracoordinate rather than pentacoordinate copper(II) center. The DFT(ADF) optimized geometry of $[\text{Cu}^{\text{I}}(\text{mb})_2]^+$ reasonably reproduces the essential features of the experimental structure of $[\text{Cu}^{\text{I}}(\text{mmb})_2](\text{BF}_4)$ (Table 2). The DFT(ADF) optimization overestimates the Cu–N and Cu–S bond lengths by a few percent; the bond lengths within the ligand part of the complex are reproduced with ± 0.02 Å accuracy.

The one-electron scheme of $[\text{Cu}^{\text{I}}(\text{mb})_2]^+$ as calculated by the DFT(ADF) method is shown in Figure 4. Molecular orbitals of a and b symmetry are characterized by antisymmetrical or symmetrical combinations of contributing ligand orbitals, respectively. The highest molecular orbitals 34a and 33b of this complex are mainly formed by combinations of d orbitals of the Cu atom with p orbitals of S, providing electron density for the “open” coordination site (Figure 5). The HOMO (34a) is calculated with 59.3% d and 6% s orbital contributions from the Cu atom and with 21.7% p orbital contributions from the S

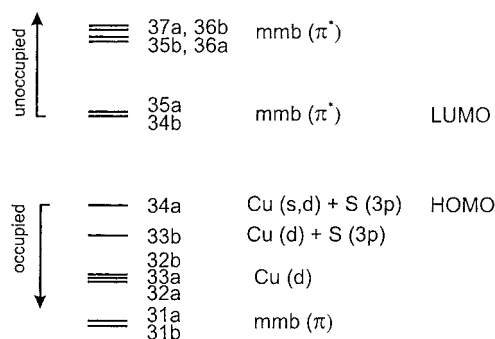


Figure 4. Molecular orbital scheme for $[\text{Cu}^{\text{I}}(\text{mb})_2]^+$ as calculated by the DFT-ADF method.

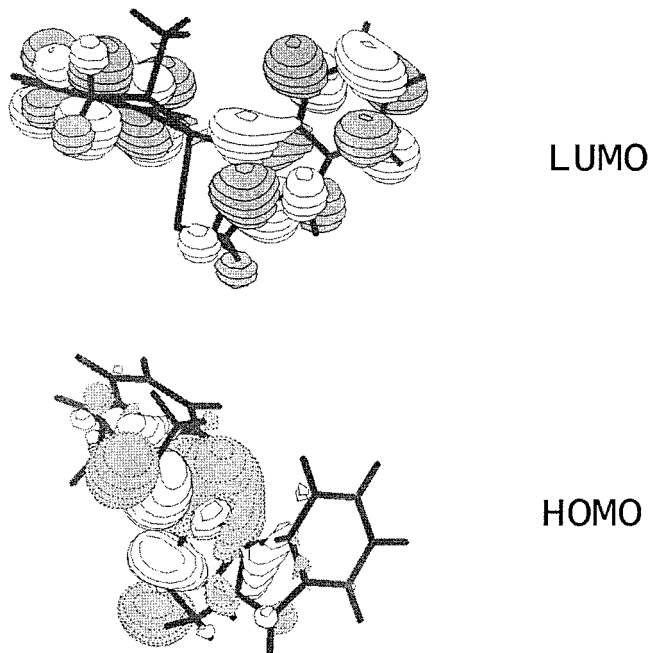


Figure 5. Composition of the LUMO and HOMO of $[\text{Cu}^{\text{I}}(\text{mb})_2]^+$.

atom. The lower lying orbital 33b is composed from 61% d orbitals of the Cu center and 30.5% p orbitals of the S atom. The lower lying set of occupied MOs is metal-localized (more than 80% Cu contribution). The lowest lying unoccupied molecular orbitals 35a and 34b are composed from π^* orbitals of the ligand with less than 1.5% contribution from the Cu atom. The HOMO and LUMO of $[\text{Cu}^{\text{I}}(\text{mb})_2]^+$ are depicted in Figure 5.

The withdrawing of an electron from $[\text{Cu}^{\text{I}}(\text{mb})_2]^+$ mainly affects the S–Cu–S fragment of the complex. The Cu atom is then accessible to further coordination, due to the character of the singly occupied MO (SOMO), the modified former HOMO of $[\text{Cu}^{\text{I}}(\text{mb})_2]^+$. However, the Cu contribution is calculated to be lower (ca. 40%) than in the HOMO of $[\text{Cu}^{\text{I}}(\text{mb})_2]^+$, which correlates with the diminished A_{\parallel} value of 13.4 mT for $[\text{Cu}^{\text{II}}(\text{mmb})_2(\text{OCIO}_3)](\text{ClO}_4)$.⁸

The geometry optimization of the $[\text{Cu}^{\text{II}}(\text{mb})_2(\text{ClO}_4)]^+$ and $[\text{Cu}^{\text{II}}(\text{mb})_2]^{2+}$ complex ions reveals hardly any variation of the ligand part of the system in comparison with $[\text{Cu}^{\text{I}}(\text{mb})_2]^+$, in agreement with the experiment using mmb. In contrast, the region close to the copper center is strongly influenced by the change of charge and the coordination of ClO_4^- (Table 2). There is a better agreement of the experimental structure data of the copper(II) compound with the bond lengths calculated for $[\text{Cu}^{\text{II}}(\text{mb})_2]^{2+}$ because the interaction with the perchlorate is

(12) (a) Fonseca Guerra, C.; Snijders, J. G.; te Velde, G.; Baerends, E. J. *Theor. Chem. Acc.* **1998**, *99*, 319. (b) Baerends, E. J.; Bérces, A.; Bo, C.; Boerrigter, P. M.; Cavallo, L.; Deng, L.; Dickson, R. M.; Ellis, D. E.; Fan, L.; Fischer, T. H.; Fonseca Guerra, C.; van Gisbergen, S. J. A.; Groeneveld, J. A.; Griitsenko, O. V.; Harris, F. E.; van den Hoek, P.; Jacobsen, H.; van Kessel, G.; Kootstra, F.; van Lenthe, E.; Onsinga, V. P.; Philipsen, P. H. T.; Post, D.; Pye, C. C.; Ravenek, W.; Ros, P.; Schipper, P. R. T.; Schreckenbach, G.; Snijders, J. G.; Sola, M.; Swerhone, D.; te Velde, G.; Vernooijs, P.; Versluis, L.; Visser, O.; van Wezenbeek, E.; Wiesenekker, G.; Wolff, S. K.; Woo, T. K.; Ziegler, T. *ADF 1999.01*; Amsterdam, 1999.

obviously overestimated. On the other hand, the angles are better reproduced (Table 2) by the calculations of $[\text{Cu}^{\text{II}}(\text{mb})_2(\text{OCIO}_3)]^+$ which take ligand/ligand interactions better into account.

Summarizing, the structural response to the reversible $\text{Cu}^{\text{I}}\text{N}_2\text{S}_2/\text{Cu}^{\text{II}}\text{N}_2\text{S}_2$ transition in the simple and geometrically rather *unrestrained* $[\text{Cu}(\text{mmb})_2]^{n+}$ complex system involves changes in the Cu–S bonding, especially of the S–Cu–S angle, whereas the almost linear N–Cu–N backbone remains virtually unchanged. The effects are reproduced by DFT calculations albeit with varying accuracy. The results thus confirm the special role of S donors in facilitating reversible electron transfer, even in the absence of electronically stronger interacting^{2,3} thiolate sulfur centers or sophisticated oligodentate ligands. The new $[\text{Cu}^{\text{I}}(\text{mmb})_2](\text{BF}_4)$ complex contains a cation with an unusual coordination geometry, involving a large and, in the crystal, channel-forming vacant site at the d^{10} metal center.

Experimental Section

Instrumentation. ¹H- and ¹³C NMR spectra were taken on a Bruker AC 250 spectrometer. UV/vis/near-IR absorption spectra were recorded on Shimadzu UV160 and Bruins Instruments Omega 10 spectrophotometers. Cyclic voltammetry was carried out at a scan rate of 100 mV/s in dichloromethane/0.2 M Bu_4NPF_6 using a three-electrode configuration (glassy carbon electrode, Pt counter electrode, Ag/AgCl reference) and a PAR 273 potentiostat and function generator. The ferrocene/ferrocenium couple served as internal reference.

Synthesis of $[\text{Cu}(\text{mmb})_2](\text{BF}_4)$. A solution of 100 mg (0.52 mmol) of mmb in 50 mL of acetone was added to 81.8 mg (0.26 mmol) of $[\text{Cu}(\text{CH}_3\text{CN})_4](\text{BF}_4)$ and stirred for 30 min at room temperature under an argon atmosphere. After reduction of the solution to about 15 mL and cooling to 4 °C, a colorless, partially crystalline and highly air-sensitive precipitate was obtained and dried to yield 118 mg (85%). Calcd for $\text{C}_{20}\text{H}_{24}\text{BCuF}_4\text{N}_4\text{S}_2$ (534.90): C, 44.91; H, 4.52; N, 10.47. Found: C, 44.98; H, 4.52; N, 10.14. ¹H NMR (acetone-*d*₆): δ = 2.45 (s, 6H, SCH_3), 4.04 (s, 6H, NCH_3), 4.50 (s, 4H, CH_2SCH_3), 7.27–7.44 (m, 4H, arom), 7.58–7.61 (m, 2H, arom), 7.70–7.73 (m, 2H, arom). ¹³C NMR (acetone-*d*₆, assignment based on DEPT 135 spectroscopy): δ = 19.20 (SCH_3), 31.08 (NCH_3), 32.12 (CH_2SCH_3), 111.76, 118.96 (C-5,6), 124.19, 124.63 (C-4,7), 137.34, 140.59 (C-3a,7a), 155.08 (C-2).

Single crystals of $[\text{Cu}(\text{mmb})_2](\text{BF}_4)$ as obtained from the reaction solution were immersed in Nujol. Measurements were performed for a colorless block (0.4 × 0.4 × 0.6 mm) on a Siemens P4 diffractometer (Table 1); cell constants were obtained with 65 reflections ($10^\circ \leq 2\Theta \leq 25^\circ$), ω -scan; 3651 reflections were collected ($4^\circ \leq 2\Theta \leq 58^\circ$, $-1 \leq h \leq 25$, $-1 \leq k \leq 13$, $-17 \leq l \leq 16$), of which 3027 are independent and 2235 have $I_o \geq 2\sigma(I_o)$, 194 parameters. Empirical absorption correction (Ψ -scan, $0.74 < T < 1.00$). The structure was solved by direct methods, and refinement on F^2 was carried out (SHELXTL 5.1);¹³ hydrogen atoms were refined freely with isotropic temperature factors, and anisotropic temperature factors were used for all other atoms. GOF = 1.026; min/max remaining electron densities $-0.470/0.472 \text{ e } \text{\AA}^{-3}$.

Calculation Procedures. In all calculations the CH_3 group attached to N in mmb was replaced by a hydrogen atom (ligand mb). Ground state electronic structure calculations of the $[\text{Cu}(\text{mb})_2]^+$, $[\text{Cu}(\text{mb})_2]^{2+}$, and $[\text{Cu}(\text{mb})_2(\text{ClO}_4)]^+$ complex ions have been done by density functional theory (DFT) methods using the ADF-1999¹² program package.

Within the ADF program Slater type orbital (STO) basis sets of double- ζ quality with polarization functions for H, B, C, N, O, F, and Cl atoms and triple- ζ quality with one additional polarization function for Cu and S were employed. Inner shells were represented by the frozen core approximation (1s for B, C, N, O, F; 1s–2p for S and Cl; 1s–3s for Cu). Within ADF the functional including Becke's gradient correction¹⁴ to the local exchange expression in conjunction with Perdew's gradient correction¹⁵ to local density approximation (LDA) with VWN parametrization of electron gas data (ADF-BP) was used.

Calculations on $[\text{Cu}(\text{mb})_2]^+$ and $[\text{Cu}(\text{mb})_2]^{2+}$ were done in constrained C_2 symmetry, and the z axis was identified with the C_2 axis.

Acknowledgment. This work was supported by Deutsche Forschungsgemeinschaft, Volkswagenstiftung, and Fonds der Chemischen Industrie.

Supporting Information Available: X-ray crystallographic files, in CIF format, for $[\text{Cu}(\text{mmb})_2](\text{BF}_4)$. This material is available free of charge via the Internet at <http://pubs.acs.org>.

IC000021U

(13) SHELXTL 5.1; Bruker Analytical X-ray Systems: Madison, WI, 1998.

(14) Becke, A. D. *Phys. Rev. A* **1988**, *38*, 3098.

(15) Perdew, J. P. *Phys. Rev. A* **1986**, *33*, 8822.